Introducing Uncertainty Components in Locational Marginal Prices for Pricing Wind Power and Load Uncertainties

Xin Fang , *Senior Member, IEEE*, Bri-Mathias Hodge , *Senior Member, IEEE*, Ershun Du , *Student Member, IEEE*, Chongqing Kang , *Fellow, IEEE*, and Fangxing Li , *Fellow, IEEE*

Abstract—**With substantially increasing penetration levels of wind power, electric power system flexibility is needed to address the variability and uncertainty of wind power output. Thus, it has become an urgent issue to obtain an optimal tradeoff between economics and reliability, and to price system uncertainties. This paper proposes a new electricity market-clearing mechanism based on locational marginal prices (LMPs) for pricing uncertain generation and load. The uncertainty contained locational marginal price (U-LMP) is derived from a distributionally robust chance-constrained optimal power flow model in which only the first-order and second-order moments of the uncertain sources' probability distribution are needed. Compared with traditional LMPs, the proposed U-LMP formulation includes two new uncertainty components: transmission line overload uncertainty price and generation violation uncertainty price. These LMP uncertainty components are the price signals reflecting the system costs as a result of wind generation and demand uncertainty at different locations. Finally, using parametric case studies, the relationship among uncertainty levels, system generation cost, and LMP uncertainty components are established. Case studies performed on the PJM 5-bus and IEEE 118-bus systems verify the proposed U-LMP method.**

Index Terms—**Economic dispatch, locational marginal price (LMP), uncertainty, optimal power flow, chance constrained optimization.**

NOMENCLATURE

c_i	Bid price of generator at Bus i($/MW·h).
G_i	Generation power output of generator at Bus i (MW).
D_i	Demand quantity (MW) at Bus i.

P_i	Wind power output (MW) at Bus i.
GSF_{l-i}	Generation shift factor of Bus i to Line l.
LU_l	Line limit of Line l.
$G_{\exp,i}$	Generation output at Bus i for expected wind power output (MW).
$P_{\exp,i}$	Expected power output (MW) of wind power plant (WPP) at Bus i.
$D_{\exp,i}$	Expected demand quantity (MW) at Bus i.
$G_i^{\max}, G_i^{\min}$	Maximum and minimum power output of generator at Bus i (MW).
β_i	Generation balancing factor for the system uncertainty.
ΔG_i	Generation response to balance the system uncertainty.
ΔP_i	Uncertain wind power output.
ΔD_i	Uncertain demand quantity.
$\xi_{w,i}$	Ratio of the standard deviation of wind power output to its expected power output.
$\xi_{d,i}$	Ratio of the standard deviation of demand to its expected value.
ϵ	Confidence level in the chance constraints.
PF_l	Power flow on transmission line l (MW).
$\gamma_{w,i,j}$	Correlation coefficient between WPPs i and j.
$\gamma_{d,i,j}$	Correlation coefficient between load i and j.
$\mu_{w,k}$	Mean of the forecast error for WPP k.
$\mu_{d,k}$	Mean of the forecast error for load k.
$\sigma_{w,k}$	Standard deviation of the forecast error for WPP k.
$\sigma_{d,k}$	Standard deviation of the forecast error for load k.
$\sigma_{PF,l}$	Standard deviation of the line power flow.
$\eta_{PF,l}$	Ancillary variable for transmission power flow standard deviation.
$\eta_{g,i}$	Ancillary variable for generation output standard deviation.
$\sigma_{g,i}$	Standard deviation of the generation power output.
λ	Dual variable of the system power balance equation.
$\mu_l^{\max}, \mu_l^{\min}$	Dual variables of the transmission upper and lower limits constraints.
$\omega_i^{\min}, \omega_i^{\max}$	Dual variables of the generation upper and lower bounds.

$\rho_{PF,l}$ Dual variable of the transmission line power flow risk component constraint.

$\varphi_{g,i}$ Dual variable of the generation power output uncertainty component constraint.

The other variables will be explained in the manuscript.

I. INTRODUCTION

RECENTLY, renewable generation, such as wind and solar, has been substantially increasing in power systems worldwide because of environmental concerns such as greenhouse gas emission, and their decreasing investment costs through technology developments [1]. In the United States, the U.S. Department of Energy target of renewable integration is to provide 20% of energy with wind at the end of 2030 [2]. Consequently, electricity markets managed by independent system operators (ISOs) have been accommodating significant wind percentage growth in terms of the generation portfolio capacity procurement. The Electric Reliability Council of Texas, Midcontinent Independent System Operator (MISO), and California Independent System Operator (CAISO) are the top three ISO-managed markets with the highest levels of wind penetration in the United States [3].

Locational marginal pricing (LMP) is a market-clearing mechanism that is a dominant approach used to determine optimal generation dispatch and energy prices by locations in the United States. This mechanism has been implemented at a number of ISOs, such as PJM, New York Independent System Operator, ISO New England, CAISO, MISO, New Zealand, and others [4]–[8].

Traditionally, LMPs are derived from the security-constrained economic dispatch (SCED) model, which can be formulated as an optimal power flow (OPF) model based on DCOPF models. The power losses can be included in DCOPF model based on different methods such as the distribution factors shown in [9]. Then, LMPs are decomposed into three components, including marginal energy price, marginal congestion price, and marginal loss price [9]–[13]. In [14], a risk-based LMP model with the risk component as a price signal representing the system's overall security level was proposed. The risk components in this model were the price signal for the system transmission overloading under normal state and contingency conditions. The reserve price for the N-1 contingency was proposed in [15]–[17] in which the reserve and energy markets are co-optimized. In these models, the uncertainties of the input generation and load are not modeled, and the system security was represented by the transmission overload level under normal and N-1 contingency states. In [18], the uncertainty marginal price was derived from a robust optimization model to co-optimize the energy and reserve capacity in the day-ahead market considering interval uncertainty input using the average-up or -down interval of the variable generation or loads. This model was based on robust optimization, and the uncertainty set for the variable generation and load was critical to obtain the reserve.

To maintain system reliability with variable renewable generation resources, chance-constrained optimal power flow (CC-OPF) has been deployed in the security constrained economic dispatch (SCED) [19]–[21]. In CC-OPF, the system transmission network power flow limits and generation output constraints are modeled to represent the impacts of load and variable generation uncertainties on the network overloading and generation violation probabilities [22]–[25]. In [23], the system reserve was procured based on the CC-OPF model to maintain the system reliability at a given risk level. Distributionally robust CC-OPF model was proposed in [26]–[29] in which only the mean and covariance of the forecast errors or the Wasserstein ambiguity set were used. This distributional robust solution might lead to an over-conservative generation dispatch with high operating cost because the results are robust to any possible distribution of the forecast errors. Robust optimization and stochastic optimization are also applied in the unit commitment and SCED problems in [30]–[34]. In robust optimization, the worst-case scenario in the predefined uncertainty sets using the average up or down intervals for the uncertainty sources such as demand or variable generation is used to maintain system reliability [35]. In stochastic optimization, a set of probabilistic scenarios represents the uncertainty. The system should maintain reliability under these scenarios which might lead to a high computation burden when the number of scenarios is large.

These models maintain system reliability level by considering the uncertainty of load or variable generation power outputs, but they do not give the price signals associated with the uncertainty levels of the variable generation and load. The system reserve cost is paid by the system load regardless of their uncertainty levels. In other words, these models cannot provide the LMPs under different uncertainty levels. While in the system, a generation or load with higher uncertainty levels leads to a higher system cost because a larger amount of flexibility resources should be procured to mitigate their uncertainty. In this case, the generation or load with higher uncertainty levels should be paid less or pay more considering their uncertainty cost. Therefore, it is important to obtain the price signals to represent the uncertainty levels, especially under high penetration levels of renewable generation.

To overcome the aforementioned disadvantages and give the price signals associated with the uncertainty levels of input wind and load, first a distributionally robust chance-constrained optimal power flow (DRCC-OPF) model is proposed which can control the constraints violation levels. In this model, only the first- and second-order moments of the forecast errors for wind power and load are needed, which are obtained from historical data instead of the predefined uncertainty sets. The transmission power flow limits and generation output constraints are modeled as chance constraints in which an adjustable coefficient controls the robustness of the chance constraints to the forecast errors. Then, the LMP uncertainty components for the transmission overloading and the generation violations are derived from the Lagrangian function of the proposed DRCC-OPF model. These uncertainty components in the LMP represent the marginal contribution of the uncertainty in variable sources such as wind power and load on the system cost. The major contributions of this paper are:

1) It extends the current LMP formulation to include two uncertainty components, resulting from the variable generation and load forecasting uncertainties.

2) The uncertainty contained LMPs (U-LMPs) are decomposed to four components similar to the current LMP formulation to give the price signals associated with the uncertainty levels of variable generation and load forecasting.

3) It proposes an DRCC-OPF model that can control the robustness of the chance constraints in the forecast error to tradeoff between economics and system security.

The rest of this paper is organized as follows: Section II presents the DRCC-OPF model, the formulation into the quadratically constrained programming (QCP) model, and the adjustable coefficient to control the distributional robustness of the chance constraints to the forecast errors distributions; Section III derives the U-LMP uncertainty components for uncertain demand and wind power; Section IV performs the case studies on the PJM 5-bus and the IEEE 118-bus systems to verify the proposed method. Section V concludes the paper.

II. DRCC-OPF

The traditional SCED model is formulated in (1a)–(1e) considering wind power and demand point forecast values to minimize the system total generation cost:

$$\min \sum_{i=1}^{N} c_i G_{exp,i} \tag{1a}$$

$$\sum_{i=1}^{N} (G_{exp,i} + P_{exp,i}) - \sum_{i=1}^{N} D_{exp,i} = 0 : \lambda \tag{1b}$$

$$\sum_{i=1}^{N} GSF_{l-i} (G_{exp,i} + P_{exp,i} - D_{exp,i}) \leq LU_l : \mu_l^{\max} \tag{1c}$$

$$- LU_l \leq \sum_{i=1}^{N} GSF_{l-i} (G_{exp,i} + P_{exp,i} - D_{exp,i}) : \mu_l^{\min} \tag{1d}$$

$$G_i^{\min} \leq G_{exp,i} \leq G_i^{\max} : \omega_i^{\min}, \omega_i^{\max} \tag{1e}$$

Then the LMP π_i is the partial derivative of the Lagrangian function of model (1) to the demand at But i [9], [36] and can be given by:

$$\pi_i = \lambda + \sum_{l=1}^{M} GSF_{l-i} \left(\mu_l^{\min} - \mu_l^{\max} \right) \tag{2}$$

When the uncertainties of load and wind power forecasts are taken into consideration, the CC-OPF model is given by the following model:

$$\min \sum_{i=1}^{N} c_i G_{exp,i} \tag{3a}$$

$$\text{s.t.} \sum_{i=1}^{N} (G_{exp,i} + P_{exp,i}) - \sum_{i=1}^{N} D_{exp,i} = 0 : \lambda \tag{3b}$$

$$\mathbf{Pr} \left(\sum_{i=1}^{N} GSF_{l-i} (G_i + P_i - D_i) \leq LU_l \right) \geq 1 - \epsilon : \mu_l^{\max} \tag{3c}$$

$$\mathbf{Pr} \left(-LU_l \leq \sum_{i=1}^{N} GSF_{l-i} (G_i + P_i - D_i) \right) \geq 1 - \epsilon : \mu_l^{\min} \tag{3d}$$

$$\mathbf{Pr} \left(G_i \leq G_i^{\max} \right) \geq 1 - \epsilon : \omega_i^{\max} \tag{3e}$$

$$\mathbf{Pr} \left(G_i^{\min} \leq G_i \right) \geq 1 - \epsilon : \omega_i^{\min} \tag{3f}$$

$$G_i = G_{exp,i} + \Delta G_i \tag{3g}$$

$$P_i = P_{exp,i} + \Delta P_i \tag{3h}$$

$$D_i = D_{exp,i} + \Delta D_i \tag{3i}$$

$$\Delta G_i = \beta_i \left(-\sum_{i=1}^{N} \Delta P_i + \sum_{i=1}^{N} \Delta D_i \right) \tag{3j}$$

$$\sum_{i=1}^{N} \beta_i = 1 \tag{3k}$$

where (3c)–(3f) are the chance constraints considering the impact of the wind and load uncertainty on the transmission overloading and generation output violation; from (3k) the total generation response equals the total wind and load power deviation which means that the power balance equation will be maintained considering the uncertainty; the variables on the right side of the colons are the dual variables of the constraints on the left side of the colons; the decision variables are $G_{exp,i}$ and β_i in this model.

For the transmission constraints in (3c) and (3d), the power flow can be formulated considering Eq. (3g) to (3j):

$$
\begin{aligned}
PF_l &= \sum_{i=1}^{N} GSF_{l-i} (G_i + P_i - D_i) \\
&= \sum_{i=1}^{N} GSF_{l-i} \left[G_{exp,i} + \beta_i \left(-\sum_{j=1}^{N} \Delta P_j + \sum_{j=1}^{N} \Delta D_j \right) \right. \\
&\quad \left. + P_{exp,i} + \Delta P_i - D_{exp,i} - \Delta D_i \right]
\end{aligned} \tag{4}
$$

The transmission line power flow, PF_l, is also random, and its uncertain part is formulated as in (5).

$$
\begin{aligned}
\sum_{i=1}^{N} GSF_{l-i} &\left[\beta_i \left(-\sum_{j=1}^{N} \Delta P_j + \sum_{j=1}^{N} \Delta D_j \right) + \Delta P_i - \Delta D_i \right] \\
&= \sum_{i=1}^{N} \left[\left(-\sum_{k=1}^{N} GSF_{l-k} \beta_k + GSF_{l-i} \right) \Delta P_i \right. \\
&\quad \left. + \left(\sum_{k=1}^{N} GSF_{l-k} \beta_k - GSF_{l-i} \right) \Delta D_i \right]
\end{aligned} \tag{5}
$$

Assume that the uncertain part of wind power output $\Delta \boldsymbol{P}$ has the mean μ_{w} and the covariance $\boldsymbol{\Sigma_w}$ shown in Eq. (9), and the uncertain part of load $\Delta \boldsymbol{D}$ has the mean μ_{d} and the covariance $\boldsymbol{\Sigma_d}$ shown in Eq. (10). Then, the standard deviation of the power flow can be rewritten as Eq. (6).

$$\sigma_{PF,l} = \sqrt{\boldsymbol{a}_{l,w} (\boldsymbol{\beta})^T \boldsymbol{\Sigma_w} \boldsymbol{a}_{l,w} (\boldsymbol{\beta}) + \boldsymbol{a}_{l,d} (\boldsymbol{\beta})^T \boldsymbol{\Sigma_d} \boldsymbol{a}_{l,d} (\boldsymbol{\beta})} \tag{6}$$

where $\sigma_{PF,l}$ is the standard deviation of the transmission power flow considering the load and wind power uncertainty, and $\boldsymbol{a}_{l,w}(\boldsymbol{\beta})$, $\boldsymbol{a}_{l,d}(\boldsymbol{\beta})$ are a one-column matrix given by Eq. (7) and (8) which are derived from Eq. (5).

$$a_{l,w,i}(\boldsymbol{\beta}) = -\sum_{k=1}^{N} GSF_{l-k}\beta_k + GSF_{l-i} \tag{7}$$

$$a_{l,d,i}(\boldsymbol{\beta}) = \sum_{k=1}^{N} GSF_{l-k}\beta_k - GSF_{l-i} \tag{8}$$

$$\boldsymbol{\Sigma}_w = \begin{bmatrix} \sigma_{w,1}^2 & \gamma_{w,1,2}\sigma_{w,1}\sigma_{w,2} \\ \gamma_{w,1,2}\sigma_{w,1}\sigma_{w,2} & \sigma_{w,2}^2 \end{bmatrix} \tag{9}$$

$$\boldsymbol{\Sigma}_d = \begin{bmatrix} \sigma_{d,1}^2 & \gamma_{d,1,2}\sigma_{d,1}\sigma_{d,2} \\ \gamma_{d,1,2}\sigma_{d,1}\sigma_{d,2} & \sigma_{d,2}^2 \end{bmatrix} \tag{10}$$

Therefore, (3c) and (3d) can be reformulated [37] as a linear constraints shown in Eq. (11) and (12).

$$\sum_{i=1}^{N} \left[GSF_{l-i}(G_{exp,i} + P_{exp,i} - D_i) + a_{l,w,i}(\boldsymbol{\beta})\mu_{w,i} \right. $$
$$\left. + a_{l,d,i}(\boldsymbol{\beta})\mu_{d,i} \right] + K_\epsilon \sigma_{PF,l} \leq LU_l \tag{11}$$

$$\sum_{i=1}^{N} \left[GSF_{l-i}(G_{exp,i} + P_{exp,i} - D_i) + a_{l,w,i}(\boldsymbol{\beta})\mu_{w,i} \right. $$
$$\left. + a_{l,d,i}(\boldsymbol{\beta})\mu_{d,i} \right] - K_\epsilon \sigma_{PF,l} \geq -LU_l \tag{12}$$

where K_ϵ is a coefficient on the standard deviation component and how to choose the value of K_ϵ will be introduced later.

Similarly, in (3e) and (3f), the standard deviation of the generation output is:

$$\sigma_{g,i} = \sqrt{\boldsymbol{b}_{w,i}(\boldsymbol{\beta})^T \boldsymbol{\Sigma}_{\boldsymbol{w}} \boldsymbol{b}_{w,i}(\boldsymbol{\beta}) + \boldsymbol{b}_{d,i}(\boldsymbol{\beta})^T \boldsymbol{\Sigma}_{\boldsymbol{d}} \boldsymbol{b}_{d,i}(\boldsymbol{\beta})} \tag{13}$$

where $\sigma_{g,i}$ is the standard deviation of the generation output, and $\boldsymbol{b}_i(\boldsymbol{\beta})$ is a one-column matrix shown in Eq. (14) and (15) which are derived from (3j).

$$\boldsymbol{b}_{w,i}(\boldsymbol{\beta_t}) = \underbrace{\left[-\beta_i \cdots -\beta_i \right]^T}_{NW} \tag{14}$$

$$\boldsymbol{b}_{d,i}(\boldsymbol{\beta_t}) = \underbrace{\left[\beta_i \cdots \beta_i \right]^T}_{ND} \tag{15}$$

where NW is the number of WPPs and ND is the number of loads.

Then, (3e) and (3f) can be reformulated as shown in Eq. (16) and (17).

$$G_{exp,i} + \beta_i \left(\sum_{k=1}^{ND} \mu_{d,k} - \sum_{k=1}^{NW} \mu_{w,k} \right) + K_\epsilon \sigma_{g,i} \leq G_i^{\max} \tag{16}$$

$$G_{exp,i} + \beta_i \left(\sum_{k=1}^{ND} \mu_{d,k} - \sum_{k=1}^{NW} \mu_{w,k} \right) - K_\epsilon \sigma_{g,i} \geq G_i^{\min} \tag{17}$$

Further, the equality constraints in (6) and (13) can be relaxed by adding auxiliary variables, as shown below in Eq. (18)

and (19).

$$\sqrt{\boldsymbol{a}_{l,w}(\boldsymbol{\beta})^T \boldsymbol{\Sigma}_{\boldsymbol{w}} \boldsymbol{a}_{l,w}(\boldsymbol{\beta}) + \boldsymbol{a}_{l,d}(\boldsymbol{\beta})^T \boldsymbol{\Sigma}_{\boldsymbol{d}} \boldsymbol{a}_{l,d}(\boldsymbol{\beta})} \leq \eta_{PF,l} \tag{18}$$

$$\sqrt{\boldsymbol{b}_{w,i}(\boldsymbol{\beta})^T \boldsymbol{\Sigma}_{\boldsymbol{w}} \boldsymbol{b}_{w,i}(\boldsymbol{\beta}) + \boldsymbol{b}_{d,i}(\boldsymbol{\beta})^T \boldsymbol{\Sigma}_{\boldsymbol{d}} \boldsymbol{b}_{d,i}(\boldsymbol{\beta})} \leq \eta_{g,i} \tag{19}$$

where (18) and (19) can be formulated as second-order cone constraints as:

$$\left\| \begin{bmatrix} \boldsymbol{\Sigma}_{\boldsymbol{w}}^{1/2} & \\ & \boldsymbol{\Sigma}_{\boldsymbol{d}}^{1/2} \end{bmatrix} \begin{bmatrix} \boldsymbol{a}_{l,w}(\boldsymbol{\beta}) \\ \boldsymbol{a}_{l,d}(\boldsymbol{\beta}) \end{bmatrix} \right\|_2 \leq \eta_{PF,l} : \rho_{PF,l} \tag{20}$$

$$\left\| \begin{bmatrix} \boldsymbol{\Sigma}_{\boldsymbol{w}}^{1/2} & \\ & \boldsymbol{\Sigma}_{\boldsymbol{d}}^{1/2} \end{bmatrix} \begin{pmatrix} \boldsymbol{b}_{w,i}(\boldsymbol{\beta}) \\ \boldsymbol{b}_{d,i}(\boldsymbol{\beta}) \end{pmatrix} \right\|_2 \leq \eta_{g,i} : \varphi_{g,i} \tag{21}$$

The CC-OPF model is then formulated as

$$\min \sum_{i=1}^{N} c_i G_{exp,i} \tag{22a}$$

s.t. Constraints $(3b), (7), (8), (14), (15), (20)$ and (21) (22b)

$$-\sum_{i=1}^{N} \left[GSF_{l-i}(G_{exp,i} + P_{exp,i} - D_i) + a_{l,w,i}(\boldsymbol{\beta})\mu_{w,i} \right. $$
$$\left. + a_{l,d,i}(\boldsymbol{\beta})\mu_{d,i} \right] - K_\epsilon \eta_{PF,l} \geq -LU_l : \mu_l^{\max} \tag{22c}$$

$$\sum_{i=1}^{N} \left[GSF_{l-i}(G_{exp,i} + P_{exp,i} - D_i) + a_{l,w,i}(\boldsymbol{\beta})\mu_{w,i} \right. $$
$$\left. + a_{l,d,i}(\boldsymbol{\beta})\mu_{d,i} \right] - K_\epsilon \eta_{PF,l} \geq -LU_l : \mu_l^{\min} \tag{22d}$$

$$-G_{exp,i} - \beta_i \left(\sum_{k=1}^{ND} \mu_{d,k} - \sum_{k=1}^{NW} \mu_{w,k} \right) - K_\epsilon \eta_{g,i} \geq -G_i^{\max} : \omega_i^{\max} \tag{22e}$$

$$G_{exp,i} + \beta_i \left(\sum_{k=1}^{ND} \mu_{d,k} - \sum_{k=1}^{NW} \mu_{w,k} \right) - K_\epsilon \eta_{g,i} \geq G_i^{\min} : \omega_i^{\min} \tag{22f}$$

More details about the CC-OPF can also be found in [19], [28], [38], [39].

If the forecasting error follows a Gaussian distribution [40], the value of K_ϵ can be decided by Eq. (23) at a given ϵ.

$$K_\epsilon = \Psi^{-1}(1 - \epsilon) \tag{23}$$

where $\Psi(\mathrm{x})$ is the cumulative distribution function (CDF) of the Gaussian distribution.

In the above CC-OPF model, the value of K_ϵ can be changed to control the chance constraints robustness to the wind power forecast errors as shown in Fig. 1. When the solutions are robust to the distribution uncertainty of the forecast errors, the values of K_ϵ in the DRCC-OPF model is chosen as below.

First, the assumption is that the mean and covariance of the uncertain variables are estimated based on the historical data [41]. All the possible distributions satisfying the mean and covariance values are represented as:

$$\boldsymbol{p} = \left\{ \mathbf{P} \in P_0\left(\mathbf{R}^{|v|}\right) : \mathbf{E}_{\mathbf{P}}[\omega] = \boldsymbol{\mu}, \mathbf{E}_{\mathbf{P}}[\omega\omega^T] = \boldsymbol{\Sigma} \right\} \tag{24}$$
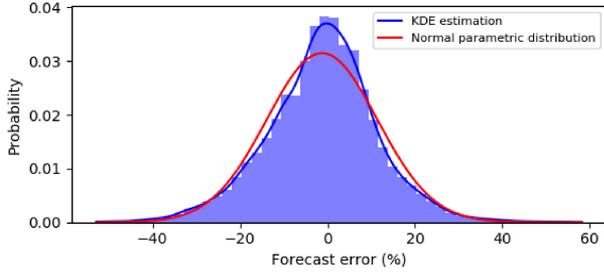
Fig. 1. Wind power forecast error distribution.

TABLE I
K_ϵ VALUES UNDER DIFFERENT DISTRIBUTION ASSUMPTIONS

ϵ	Gaussian	Sym. Dist. Robust	Dist. Robust
5%	1.645	3.1623	4.3589

where ω is the uncertain variable (here is the wind power forecast error), $P_0(\mathbf{R}^{|v|})$ represents the set of the possible probabilistic distribution on $\mathbf{R}^{|v|}$ with mean as μ and covariance matrix as Σ, and $\Sigma \in \mathbf{R}^{|v| \times |v|}$ is a positive semidefinite matrix [42].

When the mean $\hat{\mu}$ and covariance Σ of the distribution are obtained from the historical data, for $\epsilon \in (0, 1)$, the distributionally robust chance constraint is:

$$\inf_{\mu \sim (\hat{\mu}, \Sigma)} \Pr\{\mu^T \tilde{x} \le 0\} \ge 1 - \epsilon \qquad (25)$$

It is equivalent to the second-order cone constraint [37] and the value of K_ϵ is determined by Eq. (26).

$$K_\epsilon \sigma(x) + \hat{\varphi}(x) \le 0, \quad K_\epsilon = \sqrt{(1-\epsilon)/\epsilon} \qquad (26)$$

where $\tilde{x}$ is the decision variable in the chance constraints; $\sigma(x)$ is the standard deviation of the constraint; $\hat{\varphi}(\tilde{x})$ is the mean value of the constraint. Then the results will be robust to any distributions with given mean and covariance values for the forecast errors.

If the distribution is symmetrical, the distributionally robust CC-OPF is formulated [37] with the value of K_ϵ determined in Eq. (27). Then the results will be robust to any symmetric distributions with given mean and covariance values for the forecast errors.

$$K_\epsilon = \sqrt{1/2\epsilon} \qquad (27)$$

The values of K_ϵ in the three cases are listed in Table I for ϵ as 5%.

The proposed DRCC-OPF model has the adjustable coefficient (K_ϵ), which can control the robustness of the chance constraints, which may be set up for the Gaussian distribution, symmetric distributional robustness, or distributionally robust cases considering wind and load forecast uncertainty.

III. U-LMP OF THE UNCERTAIN LOAD AND WIND POWER

To obtain the U-LMP for the uncertain load and wind power, first the Lagrangian function of the model (22) is formulated:

$$L(x) = \sum_{i=1}^{N} c_i G_{exp,i} - \lambda \left(\sum_{i=1}^{N} (G_{exp,i} + P_{exp,i}) - \sum_{i=1}^{N} D_{exp,i} \right)$$
$$- \sum_{l=1}^{M} \mu_l^{\max} \left[- \sum_{i=1}^{N} GSF_{l-i} (G_{exp,i} + P_{exp,i} - D_{exp,i}) \right.$$
$$\left. - K_\delta \eta_{PF,l} + LU_l \right]$$

$$- \sum_{l=1}^{M} \mu_l^{\min} \left[\sum_{i=1}^{N} GSF_{l-i} (G_{exp,i} + P_{exp,i} - D_{exp,i}) \right.$$
$$\left. - K_\delta \eta_{PF,l} + LU_l \right]$$

$$- \sum_{i=1}^{N} \omega_i^{\max} \left(-G_i - K_\varepsilon \eta_{g,i} + G_i^{\max} \right)$$

$$- \sum_{i=1}^{N} \omega_i^{\min} \left(G_i - K_\varepsilon \eta_{g,i} - G_i^{\min} \right)$$

$$- \sum_{l=1}^{M} \rho_{PF,l} \left(\eta_{PF,l} - \left\| \begin{bmatrix} \Sigma_w^{1/2} & \\ & \Sigma_d^{1/2} \end{bmatrix} \begin{bmatrix} a_{l,w}(\beta) \\ a_{l,d}(\beta) \end{bmatrix} \right\|_2 \right)$$

$$- \sum_{i=1}^{N} \varphi_{g,i} \left(\eta_{g,i} - \left\| \begin{bmatrix} \Sigma_w^{1/2} & \\ & \Sigma_d^{1/2} \end{bmatrix} \begin{bmatrix} b_{w,i}(\beta) \\ b_{d,i}(\beta) \end{bmatrix} \right\|_2 \right) \qquad (28)$$

Then the LMP for the demand at Bus i is derived from the Lagrangian function in (28) as:

$$\frac{\partial L(x)}{\partial D_{exp,i}} = \lambda + \sum_{l=1}^{M} GSF_{l-i} \left(\mu_l^{\min} - \mu_l^{\max} \right) + \sum_{l=1}^{M} \rho_{PF,l} \frac{1}{2}$$
$$\times \frac{a_{l,d,i}^2(\beta) \xi_{d,i}^2 D_{exp,i} + a_{l,d,i}(\beta) \xi_{d,i} \sum_{j=1}^{ND} \gamma_{d,i,j} a_{l,d,j}(\beta) \xi_{d,j} D_{exp,j}}{\left\| \begin{bmatrix} \Sigma_w^{1/2} & \\ & \Sigma_d^{1/2} \end{bmatrix} \begin{bmatrix} a_{l,w}(\beta) \\ a_{l,d}(\beta) \end{bmatrix} \right\|_2}$$
$$+ \sum_{j=1}^{N} \varphi_{g,j} \frac{1}{2} \frac{\beta_j^2 \xi_{d,i}^2 D_{exp,i} + \beta_j \xi_{d,i} \sum_{j=1}^{ND} \gamma_{d,i,j} \beta_j \xi_{d,j} D_{exp,j}}{\left\| \begin{bmatrix} \Sigma_w^{1/2} & \\ & \Sigma_d^{1/2} \end{bmatrix} \begin{bmatrix} b_{w,i}(\beta) \\ b_{d,i}(\beta) \end{bmatrix} \right\|_2} \qquad (29)$$

If $\rho_{PF,l}$ is larger than 0, Constraint (20) is binding, and the following equality in Eq. (30) holds:

$$\eta_{PF,l} = \left\| \begin{bmatrix} \Sigma_w^{1/2} & \\ & \Sigma_d^{1/2} \end{bmatrix} \begin{bmatrix} a_{l,w}(\beta) \\ a_{l,d}(\beta) \end{bmatrix} \right\|_2 \qquad (30)$$

And when $\rho_{PF,l} = 0$,

$$\eta_{PF,l} > \left\| \begin{bmatrix} \Sigma_w^{1/2} & \\ & \Sigma_d^{1/2} \end{bmatrix} \begin{bmatrix} a_{l,w}(\beta) \\ a_{l,d}(\beta) \end{bmatrix} \right\|_2 \qquad (31)$$

The relationship is similar between $\varphi_{g,i}$ and (21). Then (29) is transformed as:

$$
\begin{aligned}
U\_LMP_{Load,i} &= \frac{\partial L(x)}{\partial D_{exp,i}} \\
&= \lambda + \sum_{l=1}^{M} GSF_{l-i}\left(\mu_l^{\min} - \mu_l^{\max}\right) + \sum_{l=1}^{M} \rho_{PF,l}\frac{1}{2} \\
&\times \frac{a_{l,d,i}^2(\boldsymbol{\beta})\xi_{d,i}^2 D_{exp,i} + a_{l,d,i}(\boldsymbol{\beta})\xi_{d,i}\sum_{j=1}^{ND}\gamma_{d,i,j}a_{l,d,j}(\boldsymbol{\beta})\xi_{d,j}D_{exp,j}}{\eta_{PF,l}} \\
&+ \sum_{j=1}^{N}\varphi_{g,j}\frac{1}{2}\frac{\beta_j^2\xi_{d,i}^2 D_{exp,i} + \beta_j\xi_{d,i}\sum_{j=1}^{ND}\gamma_{d,i,j}\beta_j\xi_{d,j}D_{exp,j}}{\eta_{g,i}}
\end{aligned}
$$
(32)

The third and the fourth parts of the U-LMP formulation in (32) are the prices associated with the transmission overload and generation violation because of the uncertainties. For instance, the third term is the price of the load uncertainty to the transmission overload (U-LMP_PF). The last part is the price of the load uncertainty to the generation violation (U-LMP_G). It also can be observed that if the load at Bus i has no uncertainty, such as $\xi_{d,i} = 0$, the load on Bus i does not need to pay the uncertainty price because the third and the fourth components are 0 under this circumstance. If the load reduces its uncertainty level (decreasing $\xi_{d,i}$), the uncertainty prices will also be reduced from Eq. (32). Therefore, the load will have the incentive to manage its own uncertainty level.

The total load payment to the ISOs is the product of U_LMP_{Load} and the load amount. This payment can be decomposed into two parts: energy payment and flexible reserve payment. The energy payment is the load amount multiplied by $\lambda + \sum_{l=1}^{M} GSF_{l-i}(\mu_l^{\min} - \mu_l^{\max})$. The flexible reserve payment is the load amount multiplied by (U-LMP_PF+U-LMP_G). The total load payment is the summation of the energy payment and the flexible reserve payment.

In addition, the price paid to the variable generation, such as WPPs, at Bus i is:

$$
\begin{aligned}
\frac{\partial L(x)}{\partial P_{exp,i}} &= -\lambda - \sum_{l=1}^{M} GSF_{l-i}\left(\mu_l^{\min} - \mu_l^{\max}\right) + \sum_{l=1}^{M} \rho_{PF,l}\frac{1}{2} \\
&\times \frac{a_{l,w,i}^2(\boldsymbol{\beta})\xi_{w,i}^2 P_{exp,i} + a_{l,w,i}(\boldsymbol{\beta})\xi_{w,i}\sum_{j=1}^{NW}\gamma_{w,i,j}a_{l,w,j}(\boldsymbol{\beta})\xi_{w,j}P_{exp,j}}{\boldsymbol{\Sigma}_{\boldsymbol{w}}^{1/2}\boldsymbol{a}_{l,w}(\boldsymbol{\beta})+\boldsymbol{\Sigma}_{\boldsymbol{d}}^{1/2}\boldsymbol{a}_{l,d}(\boldsymbol{\beta})_2} \\
&+ \sum_{j=1}^{N}\varphi_{g,j}\frac{1}{2}\frac{\beta_j^2\xi_{w,i}^2 P_{exp,i} + \beta_j\xi_{w,i}\sum_{j=1}^{ND}\gamma_{d,i,j}\beta_j\xi_{w,j}P_{exp,j}}{\left\|\boldsymbol{\Sigma}_{\boldsymbol{w}}^{1/2}\boldsymbol{b}_{w,i}(\boldsymbol{\beta})+\boldsymbol{\Sigma}_{\boldsymbol{d}}^{1/2}\boldsymbol{b}_{d,i}(\boldsymbol{\beta})\right\|_2}
\end{aligned}
$$
(33)

Then, similar to (32), the U-LMPs for WPPs are:

$$
\begin{aligned}
U\_LMP_{Wind,i} &= -\frac{\partial L(x)}{\partial P_{exp,i}} \\
&= \lambda + \sum_{l=1}^{M} GSF_{l-i}\left(\mu_l^{\min} - \mu_l^{\max}\right) - \sum_{l=1}^{M} \rho_{PF,l}\frac{1}{2} \\
&\times \frac{a_{l,w,i}^2(\boldsymbol{\beta})\xi_{w,i}^2 P_{exp,i} + a_{l,w,i}(\boldsymbol{\beta})\xi_{w,i}\sum_{j=1}^{NW}\gamma_{w,i,j}a_{l,w,j}(\boldsymbol{\beta})\xi_{w,j}P_{exp,j}}{\eta_{PF,l}} \\
&- \sum_{j=1}^{N}\varphi_{g,j}\frac{1}{2}\frac{\beta_j^2\xi_{w,i}^2 P_{exp,i} + \beta_j\xi_{w,i}\sum_{j=1}^{ND}\gamma_{w,i,j}\beta_j\xi_{w,j}P_{exp,j}}{\eta_{g,i}}
\end{aligned}
$$
(34)

Similarly, the third and the fourth parts are the price the wind generation should pay for the wind power uncertainty to the transmission overload and the generation violation. If the

wind generation has no uncertainty, such as $\xi_{w,i} = 0$, it will not pay these prices, and it will receive payment with the price $\pi_{w,i} = \lambda + \sum_{l=1}^{M} GSF_{l-i}(\mu_l^{\min} - \mu_l^{\max})$ without considering these uncertainty components. If the variable wind power reduces its uncertainty level (decreasing $\xi_{w,i}$), the uncertainty prices will also be reduced from Eq. (34). Therefore, the variable wind power will also have the incentive to manage its own uncertainty level.

The total wind power payment from the ISOs is the product of U_LMP_{Wind} and the wind power amount. This payment also can be decomposed into two parts: energy payment and the flexible reserve payment. The energy payment is the wind power amount multiplied by $\lambda + \sum_{l=1}^{M} GSF_{l-i}(\mu_l^{\min} - \mu_l^{\max})$. The flexible reserve payment is the wind power amount multiplied by (U-LMP_PF+U-LMP_G). The total wind payment is the energy payment minus the flexible reserve payment.

For traditional generation, the U-LMP paid to them does not include the uncertainty components because no uncertainty is associated with the traditional generation output in this model because we do not include generation contingency events. However, this could be included as in [15]–[17]. Therefore, the U-LMP for traditional generation is:

$$
U\_LMP_{Gen,i} = -\frac{\partial L(x)}{\partial G_{exp,i}} = \lambda + \sum_{l=1}^{M} GSF_{l-i}\left(\mu_l^{\min} - \mu_l^{\max}\right)
$$
(35)

In addition to the energy payment from $U\_LMP_{Gen,i}$, the traditional generation participating in balancing the system uncertainty will receive an additional payment for their flexibility reserve services as:

$$
\begin{aligned}
R_{flex,i} = \beta_i \sum_{j=1}^{N} \Big[&\left(U\_LMP\_PF_{D,j} + U\_LMP\_G_{D,j}\right)D_{exp,j} \\
&+ \left(U\_LMP\_PF_{W,j} + U\_LMP\_G_{W,j}\right)P_{exp,j}\Big]
\end{aligned}
$$
(36)

From Eq. (36), the revenue adequacy can be maintained because the total uncertainty revenue of generators equals the total uncertainty payments of load and WPPs.

Note that the partial derivative of the Lagrangian function to $\eta_{PF,l}$ and the optimal condition is shown below in Eq. (37). Then the relationship between $\rho_{PF,l}$ and $\mu_l^{\max}$, and $\mu_l^{\min}$ is shown in Eq. (38).

$$
\frac{\partial L(x)}{\partial \eta_{PF,l}} = \mu_l^{\max}K_\delta + \mu_l^{\min}K_\delta - \rho_{PF,l} = 0
$$
(37)

$$
\rho_{PF,l} = \mu_l^{\max}K_\delta + \mu_l^{\min}K_\delta
$$
(38)

Eq. (38) demonstrates that $\rho_{PF,l}$ has a value greater than 0 only when $\mu_l^{\max}$, or $\mu_l^{\min}$ has a value greater than 0. This means that Eq. (20) will be binding only when Eq. (22c) or Eq. (22d) is binding. This is intuitive because when Eq. (22c) and Eq. (22d) are not binding, the transmission line has enough capacity to accommodate the uncertainty. Therefore, the uncertainty price from this transmission line will be 0.
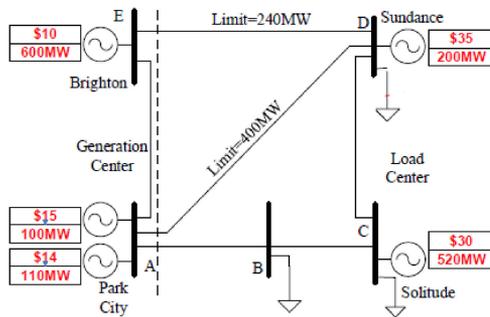
Fig. 2. PJM 5-bus system and generation parameters.

The relationship between $\varphi_{g,i}$ and $\omega_i^{\max}$, and $\omega_i^{\min}$ can be formulated in a similar way shown in Eq. (39).

$$\varphi_{g,i} = \omega_i^{\max} K_\delta + \omega_i^{\min} K_\delta \qquad (39)$$

Eq. (39) demonstrates that $\varphi_{g,i}$ has a value greater than 0 only when $\omega_i^{\max}$, or $\omega_i^{\min}$ has a value greater than 0. This means that Eq. (21) will be binding only when Eq. (22e) or Eq. (22f) is binding. When Eq. (22e) and Eq. (22f) are not binding, the generator has enough capacity to accommodate the uncertainty. Therefore, the uncertainty price from this generator will be 0.

IV. CASE STUDIES

In this section, the proposed U-LMP and DRCC-OPF model is performed on a small PJM 5-bus system to illustrate the concept and the large IEEE 118-bus system to show the application on a large system. The simulation with the proposed U-LMP model is performed in the General Algebraic Modeling System (GAMS) [43] and the MINOS solver is used to solve the proposed QCP model [44].

A. PJM 5-Bus System

The test system has been modified from the original PJM 5-bus system. The system parameters are from [45]. In this study, the peak load in this system is 1,350 MW, and the total load is equally distributed among buses B, C, and D. The system is depicted in Fig. 2. WPPs are connected to Bus B and Bus C. The wind power forecasted power outputs are 300 MW on Bus B and C. The probability ϵ in the chance constraints is 5%. The value of K_ϵ is from Table I.

B. Implication of the Uncertainty Component

In the traditional LMP model, the LMP at one node is the same for all the generation and loads connected to this node. For the system without any uncertainties from generation and load, this is true. For U-LMPs, the new uncertainty components will bring new features to the locational prices. The U-LMPs differ between different generation and loads even at the same node because of their uncertainty levels. These uncertainty components are the price signals representing the uncertainty of generation and load to the system cost.

In this subsection, the impacts of uncertainty levels of loads and generation on U-LMP results will be investigated.

TABLE II
LOAD AND WIND POWER FORECAST ERROR MEAN AND STANDARD DEVIATION

	Bus	Forecasted (MW)	σ (pu)
Load1	B	150	0
Load2	B	150	0.1
Load3	B	150	0.2
Load4	C	150	0
Load5	C	150	0.1
Load6	C	150	0.2
Load7	D	150	0
Load8	D	150	0.1
Load9	D	150	0.2
WF1	B	100	0
WF2	B	100	0.1
WF3	B	100	0.2
WF4	C	100	0
WF5	C	100	0.1
WF6	C	100	0.2
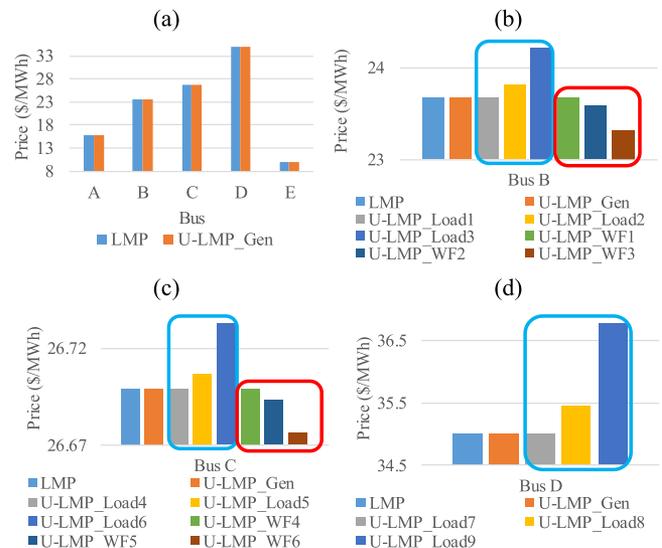
Fig. 3. LMP and U-LMP results.

Assume that the mean of forecast error is 0 and the standard deviation of load and wind forecast represents the uncertainty level and are listed in Table II. The forecast error is assumed to be Gaussian distribution. The forecast error of loads and wind are assumed to be independent. The distributional robustness will be studied in the next subsection. The LMP and U-LMP results for loads and WPPs are shown in Fig. 3. U_LMPs for loads are shown in the blue boxes and U_LMPs for wind power is shown in the red boxes in Fig. 3.

Fig. 3 demonstrates that in this case considering the chance constraints does not change the bus LMPs for the traditional generation because in Fig. 3(a) the LMPs and U-LMPs are the same. Fig. 3(b) to Fig. 3(d) show that if the load or wind generation does not have uncertainty—such as Load1, Load4, Load7 and WF1, WF4—their U-LMP will be the same as the U-LMP for the traditional generation (no uncertainty components) at the same bus; however, if the loads have uncertainty—such as Load2, Load3, Load5, Load6, Load8 and Load9—their U-LMPs increase with their uncertainty levels. This means that

TABLE III
LOAD AND WIND POWER FORECAST ERROR MEAN AND STANDARD DEVIATION

	μ (p.u.)	σ (p.u.)
Load	-0.002	0.026
WF1	-0.0646	0.2135
WF2	0.007661	0.2322

TABLE IV
U-LMPs AND SYSTEM RESULTS UNDER DIFFERENT DISTRIBUTIONS

		Gaussian	Sym. Rob.	Distr. Rob
U-LMP_Gen ($/MWh)	A	15.229	13.567	13.54
	B	22.278	18.375	18.314
	C	24.987	20.223	20.148
	D	32.438	25.305	25.193
	E	10	10	10
U-LMP_Load1 ($/MWh)		22.303	18.341	18.39
U-LMP_Load2 ($/MWh)		25.015	20.305	20.26
U-LMP_Load3 ($/MWh)		32.786	25.565	25.521
U-LMP_WF1 ($/MWh)		20.941	14.557	13.063
U-LMP_WF2 ($/MWh)		23.273	14.588	12.375
Transmission violation		5.197%	0.451%	0.0347%
Generation violation		11.47%	0.764%	0
System generation cost ($)		10868.5	12636	14074.25

TABLE V
LOAD PAYMENT AND WIND REVENUE UNDER DIFFERENT DISTRIBUTIONS

$	Gaussian		Sym. Rob.		Distr. Rob	
	Ener.	Uncer.	Ener.	Uncer.	Ener.	Uncer

the loads with higher uncertainty levels will pay more to the ISOs because their uncertainty increases the system cost. For the WPPs, their U-LMPs decrease with their uncertainty levels. Consequently, the WPPs with higher uncertainty levels will be paid less because their uncertainty is a burden to the system and increases the system operational cost.

Therefore, with the proposed U-LMPs model, both the loads and wind will be incentivized to manage their own uncertainty level, which will not only benefit their own economic concern but also improve the system reliability because the flexible reserve requirement will be reduced if loads and wind generation reduce their uncertainty levels. The measurements to reduce their uncertainty levels could include installing energy storage devices locally to smooth the output and maintain the real-time output as the forecasted values or strategically curtailing loads or wind power when the real-time values are higher than forecasted.

C. Distributional Robustness on U-LMPs

The distributional robustness is studied in this subsection. A full year of actual hourly forecast error data (8760 samples) from CAISO [46] is used as the realization of uncertain wind power output to calculate the system violations. The mean and standard deviations of loads and wind power forecast errors are shown in Table III. In this study, two WPPs are connected to Bus B and Bus C with the forecast power output of 300 MW, respectively. The total 1,350 MW load are distributed equally among Bus B, Bus C, and Bus D. The load forecast errors among three buses are independent. And the wind forecast errors between two WPPs has a positive coefficient 0.836 which is also obtained from the same CAISO data. The system U-LMPs and violations probabilities such as transmission power flow and generation output are listed in Table IV. Tables V and VI

Fig. 5.   Gen4 power output under different distributions.

Fig. 6.   Generation dispatch and balancing factors under different distributions.

TABLE VII
LOAD AND WIND POWER FORECAST ERROR MEAN AND STANDARD DEVIATION

	μ (p.u.)	σ (p.u.)
Load	-0.002	0.026
WF1	-0.0646	0.2135
WF2	0.007661	0.2322
WF3	-0.006184	0.21497
WF4	0.002075	0.2680

tributional robustness. However, the revenue from providing energy changes slightly (and increase of 5.5%) because the total energy needed in the system does not change under different distribution assumptions. The small energy cost change is because the energy provided by each generator varies under different distribution assumptions, as shown in Fig. 6(a). The distribution of the uncertainty revenue varies among different generators shown in Table VI. For instance, the uncertainty revenue of Gen1 decreases with the distributional robustness, whereas Gen5 increases this revenue tremendously. This variation of the uncertainty revenue is because of their participation in balancing the system uncertainty, as shown in Fig. 6(b). It is clear that Gen1 decreases and Gen3 and Gen5 increases the balancing factors with increasing distributional robustness. Therefore, under the U-LMP framework, the generators can receive payment for the flexible reserve service efficiently and fairly based on their participation to mitigate the system uncertainty.

Increasing the distributional robustness in the dispatch model significantly reduces the system violation regarding both the transmission power flow and generation output, whereas this distributional robustness changes both the load payments and the revenue of wind power and traditional generation, as shown in Table V and Table VI. Therefore, system operators should choose an appropriate distribution assumption to set the value of K_ϵ to control the chance constraints robustness to trade off the system security and economics.

D. IEEE 118-Bus System

The IEEE 118-bus system is studied to verify the proposed model in a large-scale system. The system data can be found in [47]–[50]. Four WPPs are connected at Bus 2, Bus 5, Bus 53, and Bus 86, and their expected power output is equal to 300 MW. The forecast error parameters of loads and WPPs are listed in Table VII. The system violation and economic results are shown in Table VIII. Fig. 7 and Fig. 8 are the transmission power flow and generation output realization considering the forecast errors. U-LMP results for WPPs, load, and traditional generators are shown in Fig. 9 to Fig. 11.

Table VIII, Fig. 7, and Fig. 8 demonstrate that considering the distributional robustness reduces the system violation for both the transmission overloading and generation output; however, this dispatch conservativeness increases the system cost. The load payment for energy does not change significantly under different distribution assumptions. While the load payment for the uncertainty increases with the robustness, but the wind payment for uncertainty decreases in the symmetric distributional-robust case. This is because in the symmetric distributional-robust and

From Fig. 4 and Fig. 5, it is obvious that both the transmission power flow and generation output changes significantly under different distribution assumptions. With higher distributional robustness, the actual violation reduces. In Fig. 4, Line 6 limit is 240 MW, and it shows that under the symmetrical distributional-robust and distributional-robust cases, the actual power flow realization reduces to less than its limit for most cases. In Fig. 5, Gen4's power output range reduces to between 0 and its maximum limit 200 MW in the distributional-robust case, which reduces its generation violation probability.

Table V shows that the load payment and wind revenue for energy reduces with the distributional robustness; however, the payment for the uncertainty increases because of their uncertainties increases the reserve requirements under higher distribution conservativeness. This is reasonable because larger amounts of reserves should be procured with higher distributional robustness for the forecast errors. Both the payment of loads and the revenue of wind show a trend to transfer from the energy service to the uncertainty components: the payment or revenue for the energy service decreases while the payment or the revenue for the uncertainty components increases with the distributional robustness.

Table VI lists the revenue of traditional generation for the energy and reserve services to mitigate the system uncertainty. The revenue from the reserve increases significantly with the distributional robustness. For instance, this revenue increases from $1,095.5 under the Gaussian distribution case to $4,139.7 under the distributional-robust case (an increase of 277.9%) because the flexible reserve requirement increases with the dis-

TABLE VIII
IEEE 118-BUS SYSTEM RESULTS UNDER DIFFERENT DISTRIBUTIONS

	Gaussian	Sym. Rob.	Distr. Rob
Transmission violation	6.423%	0.914%	0.104%
Generation violation	4.838%	1.586%	0.139%
System generation cost ($)	54,165.5	57,524.1	59,636.1
Load payment for energy	125,479.0	126,262.3	125,595.2
Load payment for uncertainty	43.0	315.1	445.4
Wind payment for energy	40,410.1	35,462.8	35,008.4
Wind payment for uncertainty	7,955.9	5,354.9	7,623.2
Gen. payment for energy	58,169.7	60,790.7	62,334.7
Gen payment for uncertainty	7,998.9	5,669.9	8,068.6

Fig. 9.   U-LMP for WPPs under different distributions.

Fig. 7.   Transmission power flow of Line 38 under different distributions.
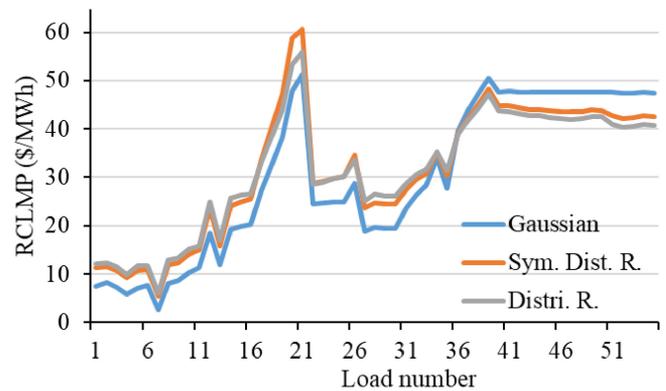
Fig. 10.   U-LMPs for loads under different distributions.

Fig. 8.   Generation output of Gen8 under different distributions.
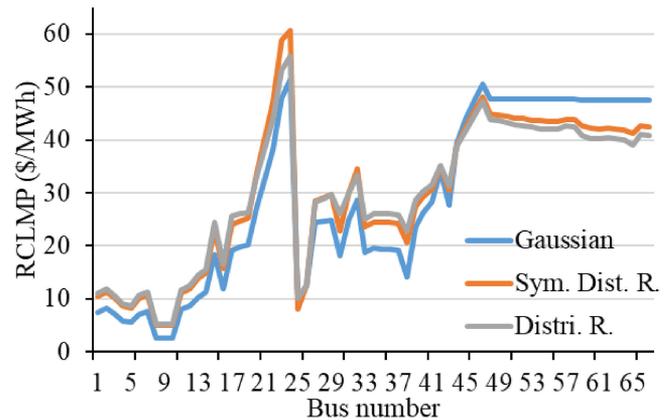
Fig. 11.   U-LMPs for traditional generators under different distributions.

the distributional-robust cases the wind curtails its power output, and therefore both the energy payment and the uncertainty payment of wind reduce.

U-LMPs for WPPs, load, and traditional generators will change with the distributional robustness, as shown in Fig 9 to Fig. 11. At some locations, these U-LMPs increase with the distributional robustness, whereas for other locations, they decrease with the conservativeness. Some loads that have small impacts on the system constraints will have the U-LMPs changes slightly under different distribution assumptions. It can be observed that U_LMPs are decided by the system risk aversion levels, the locations and uncertainty levels of load and wind power generation.

V. Conclusion

This paper proposes a U-LMP model based on a DRCC-OPF model considering wind and demand uncertainties. The U-LMP uncertainty components are derived, which demonstrate the cost

of the demand and wind uncertainty on the transmission overloading and generation violation by their locations and uncertainty levels. The system overloading and generation violation probabilities can be significantly reduced using the proposed model. The load with a higher uncertainty levels will pay more because its U-LMP increases with its uncertainty level. The wind with a higher uncertainty factor will be paid less because its U-LMP decreases with its uncertainty level. The generators that provide the flexible reserve to balance the system uncertainties can obtain a reasonable revenue for their services according to their participations and locations.

In the electricity market operation under high penetration levels of renewable generation, such as wind power, the uncertainty in the wind power and load forecasts brings challenges to system operation and leads to high LMPs because of the flexible capability shortage. Although the reserve procured in the SCED can relieve this problem, how to allocate the reserve cost efficiently and fairly is a challenge. The proposed U-LMP model offers an alternative approach to price the uncertainty of variable generation and load and compensate the generators' flexibility service. This model allocates the reserve cost to the system uncertainty sources efficiently and can maintain the system security level through the adjustable coefficient in the distributional-robust chance constraints.

Note that the U-LMP is proposed for the forward market such as the day ahead market to price the uncertainty of variable generation and demand and pay the flexible reserves of the conventional generation mitigating the uncertainty. The actual power deviation of variable generation and demand will be settled in the real time market with the real time price similar with the present two-settlement mechanism.

ACKNOWLEDGMENT

REFERENCES

[1] U.S. Department of Energy, "Staff Report to the Secretary on Electricity Markets and Reliability," 2017.

[2] U.S. Department of Energy, "20% Wind energy by 2030: increasing wind energy's contribution to US electricity supply," Energy Efficiency and Renewable Energy (EERE), 2008. [Online]. Available at: http://www.20percentwind.org/20percent_wind_energy_report_revOct08.pdf

[3] U.S. Energy Information Administration, "Form EIA-860 Annual Electric Generator Report," 2017. [Online]. Available at: https://www.eia.gov/electricity/data/eia860/

[4] "PJM training materials—LMP101." [Online]. Available at: http://www.pjm.com/training/training-material.aspx

[5] NEISO, "ISO New England's internal market monitor winter 2016 quarterly markets report," 2017.

[6] D. B. Patton, P. LeeVanSchaick, and J. Chen, "2016 state of the market report for the New York ISO markets," 2017.

[7] "2016 state of the market report for the MISO electricity market," 2017.

[8] B. B. Chakrabarti, C. Edwards, C. Callaghan, and S. Ranatunga, "Alternative loss model for the New Zealand electricity market using SFT," in Proc. IEEE Power Energy Soc. Gen. Meeting, 2011, pp. 1–8.

[9] F. Li and R. Bo, "DCOPF-based LMP simulation: Algorithm, comparison with ACOPF, and sensitivity," IEEE Trans. Power Syst., vol. 22, no. 4, pp. 1475–1485, Nov. 2007.

[10] T. Orfanogianni and G. Gross, "A general formulation for LMP evaluation," IEEE Trans. Power Syst., vol. 22, no. 3, pp. 1163–1173, Aug. 2007.

[11] A. J. Conejo, E. Castillo, R. Mínguez, and F. Milano, "Locational marginal price sensitivities," IEEE Trans. Power Syst., vol. 20, no. 4, pp. 2026–2033, Nov. 2005.

[12] J. E. Price, "Market-based price differentials in zonal and LMP market designs," IEEE Trans. Power Syst., vol. 22, no. 4, pp. 1486–1494, Nov. 2007.

[13] X. Fang, Y. Wei, and F. Li, "Evaluation of LMP intervals considering wind uncertainty," IEEE Trans. Power Syst., vol. 31, no. 3, pp. 2495–2496, May 2016.

[14] Q. Wang, G. Zhang, J. D. McCalley, T. Zheng, and E. Litvinov, "Risk-based locational marginal pricing and congestion management," IEEE Trans. Power Syst., vol. 29, no. 5, pp. 2518–2528, Sep. 2014.

[15] S. Wong and J. D. Fuller, "Pricing energy and reserves using stochastic optimization in an alternative electricity market," IEEE Trans. Power Syst., vol. 22, no. 2, pp. 631–638, May 2007.

[16] T. Zheng and E. Litvinov, "Contingency-based zonal reserve modeling and pricing in a co-optimized energy and reserve market," IEEE Trans. Power Syst., vol. 23, no. 2, pp. 277–286, May 2008.

[17] D. Gan and E. Litvinov, "Energy and reserve market designs with explicit consideration to lost opportunity costs," IEEE Trans. Power Syst., vol. 18, no. 1, pp. 53–59, Feb. 2003.

[18] H. Ye, Y. Ge, M. Shahidehpour, and Z. Li, "Uncertainty marginal price, transmission reserve, and day-ahead market clearing with robust unit commitment," IEEE Trans. Power Syst., vol. 32, no. 3, pp. 1782–1795, May 2017.

[19] L. Roald and G. Andersson, "Chance-constrained AC optimal power flow: Reformulations and efficient algorithms," IEEE Trans. Power Syst., vol. 33, no. 3, pp. 2906–2918, May 2018.

[20] H. Wu, M. Shahidehpour, Z. Li, and W. Tian, "Chance-constrained day-ahead scheduling in stochastic power system operation," IEEE Trans. Power Syst., vol. 29, no. 4, pp. 1583–1591, Jul. 2014.

[21] Y. Yuan, Q. Li, and W. Wang, "Optimal operation strategy of energy storage applied in wind power integration based on stochastic programming," IET Renew. Power Gener., vol. 5, no. 2, pp. 194–201, 2011.

[22] D. Bienstock, M. Chertkov, and S. Harnett, "Chance constrained optimal power flow: Risk-aware network control under uncertainty," pp. 1–36, 2012.

[23] T. Summers, J. Warrington, M. Morari, and J. Lygeros, "Stochastic optimal power flow based on conditional value at risk and distributional robustness," Int. J. Elect. Power Energy Syst., vol. 72, pp. 116–125, 2015.

[24] L. Roald, S. Misra, T. Krause, and G. Andersson, "Corrective control to handle forecast uncertainty: A chance constrained optimal power flow," IEEE Trans. Power Syst., vol. 32, no. 2, pp. 1626–1637, Mar. 2017.

[25] L. Roald, F. Oldewurtel, T. Krause, and G. Andersson, "Analytical reformulation of security constrained optimal power flow with probabilistic constraints," in Proc. 2013 IEEE Grenoble Conf. PowerTech, 2013, pp. 1–6.

[26] C. Duan, W. Fang, L. Jiang, L. Yao, and J. Liu, "Distributionally robust chance-constrained approximate AC-OPF with wasserstein metric," IEEE Trans. Power Syst., vol. 33, no. 5, pp. 4924–4936, Sep. 2018.

[27] M. Vrakopoulou, B. Li, and J. L. Mathieu, "Chance constrained reserve scheduling using uncertain controllable loads Part I: Formulation and scenario-based analysis," IEEE Trans. Smart Grid, vol. 10, no. 2, pp. 1608–1617, Mar. 2019.

[28] M. Vrakopoulou, B. Li, and J. L. Mathieu, "Chance constrained reserve scheduling using uncertain controllable loads part II: Analytical reformulation," IEEE Trans. Smart Grid, vol. 10, no. 2, pp. 1618–1625, Mar. 2019.

[29] L. Roald, F. Oldewurtel, B. Van Parys, and G. Andersson, "Security constrained optimal power flow with distributionally robust chance constraints," pp. 1–8, 2015. [Online]. Available: https://arxiv.org/abs/1508.06061

[30] H. Ye and Z. Li, "Robust security-constrained unit commitment and dispatch with recourse cost requirement," IEEE Trans. Power Syst., vol. 31, no. 5, pp. 3527–3536, Sep. 2016.

[31] B. Hu, L. Wu, and M. Marwali, "On the robust solution to SCUC with load and wind uncertainty correlations," *IEEE Trans. Power Syst.*, vol. 29, no. 6, pp. 2952–2964, Nov. 2014.

[32] R. Jiang, J. Wang, M. Zhang, and Y. Guan, "Two-stage minimax regret robust unit commitment," *IEEE Trans. Power Syst.*, vol. 28, no. 3, pp. 2271–2282, Aug. 2013.

[33] F. Teng, V. Trovato, and G. Strbac, "Stochastic scheduling with inertia-dependent fast frequency response requirements," *IEEE Trans. Power Syst.*, vol. 31, no. 2, pp. 1557–1566, Mar. 2016.

[34] R. Dominguez, A. J. Conejo, and M. Carrion, "Toward fully renewable electric energy systems," *IEEE Trans. Power Syst.*, vol. 30, no. 1, pp. 316–326, Jan. 2015.

[35] G. Xu and S. Burer, "A data-driven distributionally robust bound on the expected optimal value of uncertain mixed 0-1 linear programming," *Comput. Manage. Sci.*, vol. 15, no. 1, pp. 111–134, 2018.

[36] X. Fang, Q. Hu, F. Li, B. Wang, and Y. Li, "Coupon-based demand response considering wind power uncertainty: A strategic bidding model for load serving entities," *IEEE Trans. Power Syst.*, vol. 31, no. 2, pp. 1025–1037, Mar. 2016.

[37] G. C. Calafiore and L. El Ghaoui, "On distributionally robust chance-constrained linear programs," *J. Optim. Theory Appl.*, vol. 130, no. 1, pp. 1–22, 2006.

[38] M. Lubin, Y. Dvorkin, and S. Backhaus, "A robust approach to chance constrained optimal power flow with renewable generation," *IEEE Trans. Power Syst.*, vol. 31, no. 5, pp. 3840–3849, Sep. 2016.

[39] H. Zhang and P. Li, "Chance constrained programming for optimal power flow under uncertainty," *IEEE Trans. Power Syst.*, vol. 26, no. 4, pp. 2417–2424, Nov. 2011.

[40] R. A. Jabr, "Adjustable robust OPF with renewable energy sources," *IEEE Trans. Power Syst.*, vol. 28, no. 4, pp. 4742–4751, Nov. 2013.

[41] R. Jiang and Y. Guan, *Data-Driven Chance Constrained Stochastic Program*, vol. 158, no. 1–2, Berlin, Germany: Springer 2016.

[42] W. Xie and S. Ahmed, "Distributionally robust chance constrained optimal power flow with renewables: A conic reformulation," *IEEE Trans. Power Syst.*, vol. 33, no. 2, pp. 1860–1867, Mar. 2018.

[43] "GAMS," 2018. [Online]. Available at: http://www.gams.com/

[44] "MINOS," 2018. [Online]. Available: https://www.gams.com/24.8/docs/solvers/minos/index.html

[45] F. Li and R. Bo, "Small test systems for power system economic studies," in *Proc. Power Energy Soc. Gen. Meeting*, 2010, pp. 1–4.

[46] B.-M. Hodge, A. Florita, K. Orwig, D. Lew, and M. Milligan, "A comparison of wind power and load forecasting error distributions," in *Proc. World Renew. Energy Forum*, 2012, vol. 3.

[47] X. Fang, F. Li, Y. Wei, and H. Cui, "Strategic scheduling of energy storage for load serving entities in locational marginal pricing market," *IET Gener., Transmiss. Distrib.*, vol. 10, no. 5, pp. 1258–1267, 2016.

[48] "IEEE 118-bus System," 2018. [Online]. Available at: motor.ece.iit.edu/data/JEAS_IEEE118.doc

[49] X. Fang, F. Li, Q. Hu, and Y. Wei, "Strategic CBDR bidding considering FTR and wind power," *IET Gener., Transmiss. Distrib.*, vol. 10, no. 10, pp. 2464–2474, 2016.

[50] X. Fang, B.-M. S. Hodge, E. Du, N. Zhang, and F. Li, "Modelling wind power spatial-temporal correlation in multi-interval optimal power flow: A sparse correlation matrix approach," *Appl. Energy*, vol. 230, pp. 531–539, 2018.